

# The role of Coulomb interaction in fragmentation

M.J. Ison<sup>1</sup> and C.O. Dorso<sup>1</sup>

<sup>1</sup> Departamento de Física, Facultad de Ciencias Exactas y Naturales,  
Universidad de Buenos Aires, Pabellón I, Ciudad Universitaria, Nuñez, 1428,  
Buenos Aires, Argentina.\*

(Dated: November 2, 2018)

We examine the impact of adding a Coulomb term to a constrained system of 147 particles interacting via a Lennard-Jones (*LJ*) potential, finding that the inclusion of the coulombic interaction produces a shift, but no qualitative changes in the thermodynamical properties of the system. We also performed the systems characterization from a morphological point of view.

PACS numbers: 21.10.Sf, 25.70.-z, 25.70.Pq, 68.35.Rh, 02.70.Ns

The analysis of the caloric curves (*CC*) of small systems is attracting the attention of physicists in different areas. One of the most active ones is precisely nuclear physics because of the possibility of the occurrence of phase transitions in multifragmentation experiments. A wealth of theoretical and experimental work has flourished in recent years with, in some cases contradictory results. In particular a debate has recently arisen regarding the effect of Coulomb interaction on the properties of the *CC*. Whereas some authors references [1, 2] claim that there exist a loop in the *CC* denoting a negative thermal response function for systems as large as 200 particles it has also been claimed that an upper limit in the mass exist ( $A = 60$ ) [3, 4] above which no such a loop can exist. In Ref.[5] it is stated that the presence of Coulomb forbids the phase transition for systems as large as  $A = 200, Z = 82$  (a proton fraction of 0.4). On the other hand in Ref.[6] they propose a model in which  $c_v$  is never negative.

In this communication we will show that, when dealing with finite constrained systems interacting via a Lennard-Jones 6 – 12 potential which has been shown to display negative values of the specific heat [or more generally speaking, the thermal response function (*TRF*)] for low values of the density [7], the addition of the Coulomb interaction term preserve the shape of the caloric curve and gives rise to a displacement of the location of the loop together with its flattening. These results are consistent with lattice models calculations including Coulomb interaction [8]. It is worth to mention that the relevance of the analysis of *LJ* systems relies on the fact that the *EOS* of the *LJ* and the one assumed to describe nuclear matter are quite similar [9, 10].

The system under study is composed by a gas of 147 particles confined in a spherical box, defined by the Hamiltonian  $H = K + V_{LJ} + V_{coulomb} + V_{walls}$ , where  $K$  is the kinetic energy and the short-range term of the interaction potential is given by  $V_{LJ} = \Sigma v(r_{ij})$  with  $v(r_{ij}) = 4\epsilon \left[ \frac{(\sigma)}{r_{ij}}^{12} - \frac{(\sigma)}{r_{ij}}^6 \right]$  if  $(0 < r < r_c)$  and 0 otherwise

wise. In this work we took a cut-off radius  $r_c = 3.0\sigma$ , and adopted adimensional units for the energy, length and time such that  $\epsilon = \sigma = 1, t_0 = \sqrt{\sigma^2 m / 48\epsilon}$ .

The role of  $V_{walls}$  is to constrain the particles inside an spherical container. The considered external potential behaves like  $V_{wall} \sim (r - r_{wall})^{-12}$  with a cut-off distance  $r_{cut} = 1\sigma$ , where it smoothly became zero along with its first derivative.

The addition of the coulombic interaction  $V_{coulomb}$  in the hamiltonian has been done with two different approaches that will be henceforth referenced as the homogeneous and the inhomogeneous one.

The homogeneous case, which could be useful in the study of metallic clusters and has already been introduced for the study of nuclear fragmentation [9], the coulombic force is included between all particles of the fluid,  $V_{coulomb} = q^2/r_{ij}$ , with  $q^2 = 0.055$ , which was obtained in [9] by comparing the binding energy formula for argon balls with the nuclear drop mass formula assuming the proton fraction to be 0.4 (roughly speaking, it has been adjusted so that liquid argon drops having  $\sim 300$  atoms are unstable under fission).

In the second case, i.e. the inhomogeneous case, the Coulomb term is only present between a subset ( $Z$ ) of the ( $A$ ) particles which will be renamed as "protons" (the other  $A - Z$  will therefore called "neutrons"). Taking the same proton fraction as in the previous case ( $\frac{Z}{A} = 0.4$ ), we adjusted the strength of the Coulomb term so that we have the same total energy ( $E = K + V_{LJ} + V_{coulomb} + V_{walls}$ ) for the same configuration. The value of  $q^2$  turned out to be  $q^2 = 0.238$ . This last approach mimics the nuclear scenario in a more realistic way.

For both systems we have performed extensive molecular dynamics simulations following the same approach as described in [7].

We will first focus on the thermodynamics of these systems at a very low densities ( $\rho < 0.025\sigma^{-3}$ ). For these densities a pure *LJ* system displays a well defined loop in its *CC* as a direct consequence of the ability of the system to form well defined fragments in configuration space [7]. In the upper panel of Fig. 1 we show the caloric curves for a pure *LJ* (empty circles), *LJ* + *Coulomb* inhomogeneous case (full triangles) and homogeneous case (full squares)

\*Electronic address: mison@df.uba.ar

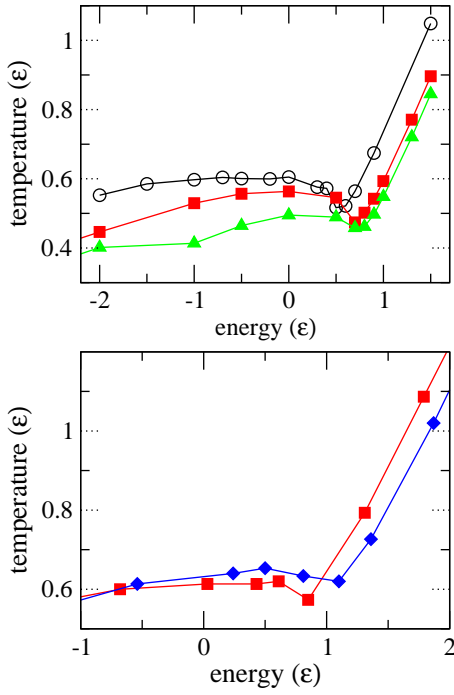


**FIG. 1:** Top:Caloric curves for  $\rho = 0.01\sigma^{-3}$ . Pure LJ (empty circles), inhomogeneous (filled squares) and homogeneous (filled triangles) systems. Bottom: Caloric curves for an inhomogeneous system with  $\rho = 0.015\sigma^{-3}$ .  $A = 147$ ,  $Z = 62$  (squares) and  $A = 294$ ,  $Z = 124$  (diamonds).

for  $\rho = 0.01\sigma^{-3}$ . It can be seen that for all the three cases a clear loop is displayed. If we restrict our analysis to the systems with Coulomb interaction we notice that the location of the minima of the loop is shifted with respect to the *LJ* case. This shift is of the order of  $0.3\epsilon$ , which corresponds to the mean coulombic energy of the system. This can be easily verified by plotting the temperature as a function of  $K + V_{LJ}$ , in which case the shift disappears denoting that the partition of the total potential energy is made into two terms: The LJ potential energy which is extremely sensitive to the presence of inner surfaces, and the coulomb term, which is, on the contrary, very insensitive due to its long range.

In the lower panel of Fig. 1 we illustrate the fact that the presence of the loop is quite resilient to an increase of the systems size. In particular we show the *CC* for  $\rho = 0.023\sigma^{-3}$  and  $A = 294$  for the pure *LJ* system and the inhomogeneous case (with  $Z = 124$ ). It can be seen that both the loop and the shift remain present.

In order to gain further insight into the properties of such a system we studied the second moments of the distribution of kinetic energies, namely the standard deviation of the kinetic energy per particle and the relative

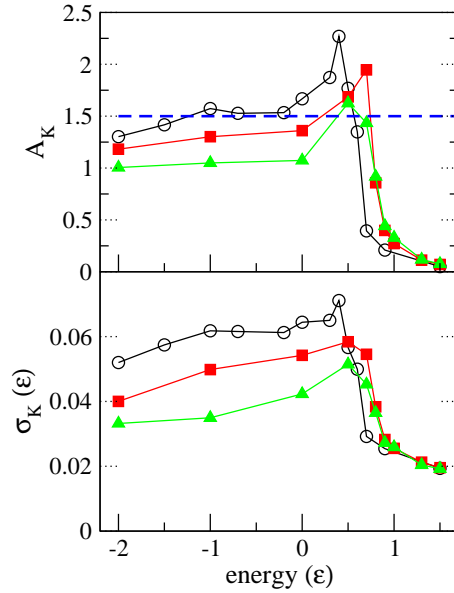


**FIG. 2:** Top:Relative fluctuations of kinetic energy for  $\rho = 0.01\sigma^{-3}$ . Pure LJ (empty circles), inhomogeneous (filled squares) and homogeneous (filled triangles) systems. Bottom: Standard deviation of kinetic energy per particle for the same cases.

kinetic energy fluctuations, defined as

$$A_K = N \frac{\sigma_K^2}{T^2} \quad (1)$$

where  $N$  is the number of particles,  $\sigma_K$  the standard deviation of the kinetic energy per particle and  $T$  the temperature of the system. Since kinetic energy fluctuations and the specific heat are related by [11]

$$N < \sigma_K^2 >_E = \frac{3}{2\beta^2} \left(1 - \frac{3}{2C}\right) \quad (2)$$

Negative values of the specific heat should be expected whenever  $A_K$  exceeds the canonical  $A_K(\text{can}) = 1.5$  [7, 12].

In Fig. 2 we show these two quantities,  $A_K$  (upper panel) and  $\sigma_K$  (lower panel). Once again the presence of the loop in the *CC* is correlated to the peaks in the values of  $A_K$  and  $\sigma_K$ . Moreover these peaks are above the canonical value (dashed line of Fig. 2) thus denoting a negative value of the *TRF*. It is also interesting to notice that for the homogeneous case the size of the peak is strongly reduced, which is in accordance with the fact that the loop in the corresponding *CC* is shallower. On the other hand for the inhomogeneous case this effect is much weaker.

Following the scheme used in reference [13] we now explore the effect of increasing the density in the above presented quantities. The results are summarized in Fig. 3 in

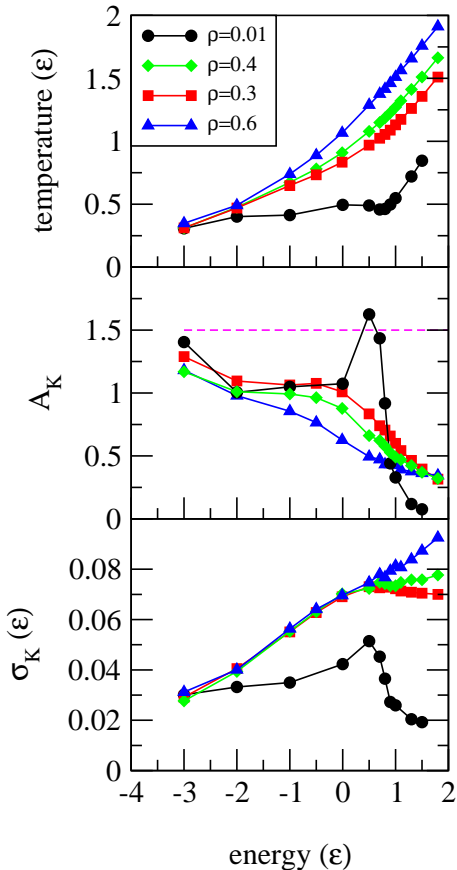


**FIG. 3:** Caloric curve for the homogeneous  $LJ + coulomb$  case for different densities (upper panel). Relative fluctuation of the kinetic energy (medium panel) (notice that the peak of  $A_K$  exceeds the 1.5 canonical value for  $\rho = 0.01\sigma^{-3}$ ). Standard deviation of the kinetic energy per particle (bottom).

which we show the temperature (upper panel),  $A_K$  (middle panel) and  $\sigma_K$  (lower panel) for different densities (see figure caption for details). In the case of the temperature it displays a transition from a  $CC$  with a loop ( $\rho = 0.01\sigma^{-3}$ ) to a monotonously increasing function for the highest density considered ( $\rho = 0.60\sigma^{-3}$ ). For intermediate density values the  $CC$  displays a change of slope. These features are in complete agreement with the already calculated behavior of the  $CC$  for the pure  $LJ$  case [13]. The behavior displayed by  $A_K$  and  $\sigma_K$  (middle and lower panels respectively) is also similar to those found for the pure  $LJ$  case. These results confirm the already pointed "triviality" of the inclusion of Coulomb interaction for small constrained systems. It is worth to mention at this point that the behavior of the unnormalized fluctuation of the kinetic energy  $\sigma_K$  changes qualitatively from displaying a loop to an increasing function of the energy at a density between  $\rho = 0.3\sigma^{-3}$  and  $\rho = 0.4\sigma^{-3}$  which has been pointed out [14] to be the critical density for an homogeneous  $LJ + Coulomb$  system.

So far the presence of Coulomb interaction has not

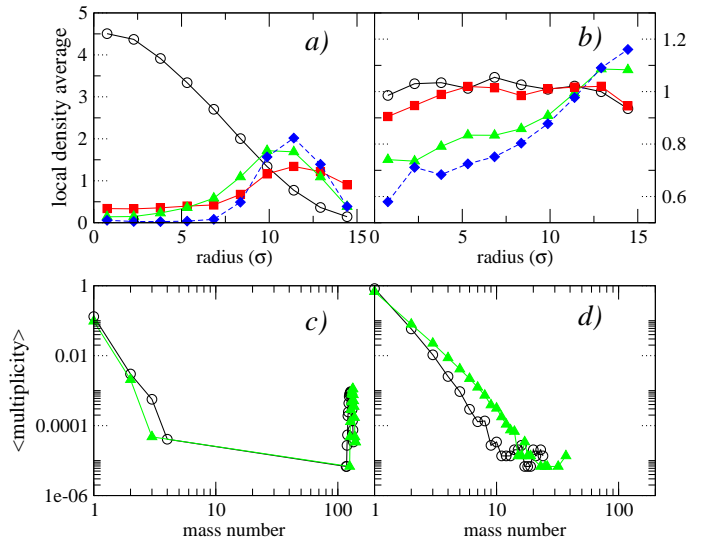


**FIG. 4:** Panels (a) and (b): Local density profiles averages (LDPA) for a liquid-like configuration (a) and a gas-like configuration (b).  $LJ$  LDPA (empty circles), homogeneous  $LJ + Coulomb$  LDPA (filled triangles), proton LDPA (filled diamonds), and neutron LDPA (filled squares). Panels (c) and (d): Mass distributions for the  $LJ$  (empty circles) and homogeneous  $LJ + Coulomb$  (filled triangles) cases.

modified any of the "thermodynamic" properties of the system. We now turn to the analysis of its morphological properties. We first study the density profiles for the three cases studied in this work. For this purpose we divide our system in concentrical equally spaced shells and calculate the normalized average populations of each shell. We have performed this analysis for the low density case for two relevant energies, namely  $E = -2.0\epsilon$  and  $E = 1.0\epsilon$  for the  $LJ + Coulomb$  systems and  $E = -2.7\epsilon$  and  $E = 0.7\epsilon$  for the  $LJ$  case (panels (a) and (b) in Fig. 4). To properly understand this behavior we have performed a fragment analysis of the system. We have defined fragments according to the following definition (see [15, 16]): Given a set of particles  $i, j, \dots, k$ , it belongs to the same cluster  $C_i$  if:

$$\forall i \in C_i, \exists j \in C_i / e_{ij} \leq V_{max} \quad (3)$$

where  $e_{ij} = V(r_{ij}) + (\mathbf{p}_i - \mathbf{p}_j)^2/4\mu$ ,  $\mu$  is the reduced mass of the pair  $\{i, j\}$ , and  $V_{max}$  is an upper limit for the potential energy (0 in the  $LJ$  case).

This definition takes into account in an approximate way the relative momentum of the particles. The corresponding mass distributions are displayed in panels (c), (d) (for the same energies depicted as before). For the sake of clarity we only show the fragment mass spectra for the pure  $LJ$  and the homogeneous case. We can see that for pure  $LJ$  and homogeneous case a big fragment is formed together with small aggregates giving rise to a U-shape distribution so the difference in the density

profiles (circles and triangles in panels (a), (b) for  $LJ$ ,  $LJ + Coulomb$  respectively) comes from the fact that the big fragment for the pure  $LJ$  case travels along the whole volume remaining mainly in the center of the container whereas for the homogeneous case it remains close to the walls due to Coulomb repulsion with the rest of the system. For the high energy case the system is mainly composed of small fragments, in both analyzed cases, but while for the pure  $LJ$  case particles are homogeneously distributed inside the volume, for the charged system the effect of repulsion gives rise to a higher density close to the walls.

Turning our attention to the inhomogeneous case, it is interesting to notice the differences between the proton and neutron density profiles (squares and diamonds in panels *a*) and *b*) of Fig. 4 respectively). For the low energy case no major differences are found, which is related to the fact that the structure of the big clusters is composed by both protons and neutrons. However, the scenario changes completely when looking at the system at high energies (panel *(b)*). Since the system is now composed mainly of small clusters the density profile of

the protons is quite similar to the homogeneous case, with higher values close to the walls due to Coulomb repulsion, but the neutron density profile now clearly resembles the  $LJ$  profile i.e. an homogeneous distribution inside the container.

To sum up, after analyzing both thermodynamical (caloric curves, kinetic energy fluctuations) and morphological properties (fragment mass distributions, density profiles) of systems with and without Coulomb interaction we came up with the result that phase transitions in small systems, with masses of the order of those relevant for the nuclear case, are not substantially modified by the presence of such long range forces. Nevertheless a slight reduction of the signals takes place specially for the homogeneous case, which could be useful in the study of metallic clusters, where negative specific heats have been measured experimentally [17].

We thank Ariel Chernomoretz for useful discussions and Francesca Gulminelli for a critical reading of the manuscript. This work was partially supported by the University of Buenos Aires via grant X139.

---

- [1] P. Chomaz, V. Duflot, and F. Gulminelli *Phys. Rev. Lett.*, vol. 85, p. 3587, 2000.
- [2] F. Gulminelli and P. Chomaz, 2003. arXiv:nucl-th/0304058.
- [3] L. G. Moretto, J. B. Elliott, L. Phair, and G. J. Wozniak *Phys. Rev. C*, vol. 66, p. 041601, 2002.
- [4] L. G. Moretto, J. B. Elliott, and L. Phair, 2003. arXiv:nucl-th/0307102.
- [5] A. H. Raduta and A. R. Raduta *Phys. Rev. Lett.*, vol. 87, p. 202701, 2001.
- [6] C. B. Das, S. D. Gupta, and A. Z. Mekjian *Phys. Rev. C*, vol. 68, p. 014607, 2003.
- [7] A. Chernomoretz, M. Ison, S. Ortíz, and C. Dorso *Phys. Rev. C*, vol. 64, p. 024606, 2001.
- [8] J. M. Carmona, J. Richert, and P. Wagner *Eur. Phys. J. A*, vol. 11, p. 87, 2001.
- [9] R. J. Lenk and V. R. Pandharipande *Phys. Rev. C*, vol. 34, p. 177, 1986.
- [10] T. J. Schlagel and V. R. Pandharipande *Phys. Rev. C*, vol. 36, p. 162, 1987.
- [11] J. L. Lebowitz, J. K. Percus, and L. Verlet *Phys. Rev.*, vol. 153, p. 250, 1967.
- [12] F. Gulminelli, P. Chomaz, and V. Duflot *Europhys. Lett.*, vol. 50, p. 434, 2000.
- [13] A. Chernomoretz, P. Balenzuela, and C. Dorso *Nucl. Phys. A*, vol. 723, p. 229, 2003.
- [14] X. Campi, H. Krivine, E. Plagnol, and N. Sator *Phys. Rev. C*, vol. 67, p. 044610, 2003.
- [15] T. Hill, *Thermodynamics of small systems*. Dover, 1994.
- [16] A. Strachan and C. O. Dorso *Phys. Rev. C*, vol. 56, p. 995, 1997.
- [17] M. Schmidt, R. Kusche, T. Hippler, J. Donges, W. Krommiller, B. von Issendorff, and H. Haberland *Phys. Rev. Lett.*, vol. 86, p. 1191, 2001.